analytical chemistry

Article

pubs.acs.org/ac

Two-Dimensional Photonic Crystal Sensors for Visual Detection of Lectin Concanavalin A

Jian-Tao Zhang,† Zhongyu Cai,† Daniel H. Kwak, Xinyu Liu,* and Sanford A. Asher*

Department of Chemistry, University of Pittsburgh, 219 Parkman Avenue, Pittsburgh, Pennsylvania 15260, United States

ABSTRACT: We fabricated a two-dimensional (2-D) photonic crystal lectin sensing material that utilizes light diffraction from a 2-D colloidal array attached to the surface of a hydrogel that contains mannose carbohydrate groups. Lectin−carbohydrate interactions create hydrogel cross-links that shrink the hydrogel volume and decrease the 2-D particle spacing. This mannose containing 2-D photonic crystal sensor detects Concanavalin A (Con A) through shifts in the 2-D diffraction wavelength. Con A concentrations can be determined by measuring the diffracted wavelength or visually determined from the change in the sensor diffraction color. The concentrations are easily monitored by measuring the 2-D array Debye ring diameter. Our observed detection limit for Con A is 0.02 mg/mL (0.7 μM). The 2-D photonic crystal sensors are completely reversible and can monitor Con A solution concentration changes.

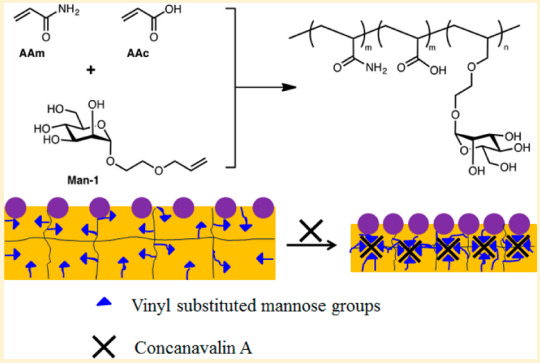

Infectious diseases caused by microbes such as bacteria, fungi, and viruses are the leading cause of death worldwide.[1] Early detection and diagnosis of microbial infections are the most effective strategies to mitigate these diseases. Thus, there is a great need for simple, inexpensive approaches to rapidly detect infectious microbes in water, food, air, and biological fluids.

The clinical chemistry detection of bacterial pathogens generally utilizes microtiter plate immunoassays. These immunoassay methods include radioimmunoassay (RIA), enzyme immunoassay (EIA), and fluoroimmunoassay (FIA) techniques.[2,3] RIA is extremely sensitive, but radiation waste storage and training of staff complicate its use. EIA is the most widely used immunoassay method. Unfortunately, its enzyme labels are bulky and are susceptible to inhibition and denaturation.[4] FIA, while simple and rapid, shows lower sensitivities.[2,3,5]

There is great interest in developing superior methods for detecting microorganisms. Many microbial pathogens infect host organisms by adhering and entering host cells through specific binding to host cell surface carbohydrates.[6] Recently, gold nanoparticles,[7] conjugated polymers[8] and carbon nanotubes[9] were functionalized with carbohydrates to mimic the multivalent carbohydrate scaffolds present in host cells. Novel electrochemical and fluorescence microscopy methods were used to monitor these assemblies to detect the target microorganisms.

We recently developed a 2-D photonic crystal (2-D PhC) sensing technology that utilizes responsive hydrogels that shift their diffraction wavelengths in response to targeted analyte concentrations.[10−15] These 2-D PhCs diffract light at wavelengths that depend on their 2-D array particle spacing. These 2-D PhC sensing materials have been developed for the visual determination of pH, ionic strength, charged surfactants, and proteins in aqueous media.[10−15] A number of recent reviews discuss hydrogel sensing PhC.[16−18]

In the work here we extend this technology to detect lectins. We demonstrate the fabrication of a carbohydrate-functionalized 2-D PhC that binds to the lectin concanavalin A (Con A), causing a diffraction wavelength shift. Specifically, we show that Con A binding to a mannose-containing 2-D PhC hydrogel actuates a hydrogel volume phase transition that decreases the particle spacing, that blue shifts the diffracted wavelength in proportion to the Con A concentration.

EXPERIMENTAL SECTION

Materials. Acrylamide (AAm), acrylic acid (AAc), *N*,*N*′-methylenebis(acrylamide) (MBAAm), 2-hydroxy-1-(4-(2-hydroxyethoxy)-phenyl)-2-methyl-1-propanone (Irgacure 2959), sodium chloride, calcium chloride dehydrate, manganese chloride tetrahydrate, and D-mannose were purchased from Sigma-Aldrich and used as received. 1-Propanol was purchased from J. T. Baker Inc. Con A, type IV, from *Canavalia ensiformis* (jack bean) was purchased from Sigma-Aldrich. Unconjugated *Ricinus communis* agglutinin I (RCA I, RCA_{120}) was purchased from Vector Laboratories, Inc. Polystyrene (PS) particles with a diameter of 580 nm were synthesized by using an emulsion polymerization as previously reported.[19] Mannose monomer (Man-1) was prepared by glycosylating 2-allyloxyethanol (TCI) with per-acetylated mannose (Carbosynth) using $BF_3{\cdot}OEt_2$ (Acros) as a catalyst, followed by saponification to remove the acetate protecting group. In brief, per-acetylated mannose (0.78 g) and 2-allyloxyethanol (0.25 g) were dissolved in dry dichloromethane (10 mL) under a nitrogen atmosphere. The solution was cooled to 0 °C, and $BF_3{\cdot}Et_2O$ (1.05 mL) was added dropwise. The reaction was stirred for

Received: April 30, 2014
Accepted: August 27, 2014
Published: August 27, 2014

   dx.doi.org/10.1021/ac5015854 | *Anal. Chem.* 2014, 86, 9036−9041

30 min at 0 °C and then overnight at room temperature. The reaction was quenched by saturated aqueous sodium bicarbonate and extracted with dichloromethane. The combined organic layer was washed further with water and brine and dried over Na_2SO_4, and the solvent was removed under reduced pressure to give the crude residue. The crude peracetylated 2-(alloxyl)ethyl mannoside was dissolved in methanol (10 mL), and anhydrous NaOMe (54 mg) was added. The mixture was heated to reflux for 6 h to allow for the complete deacetylation. Solvent was then evaporated, and the residue was purified by silica gel column chromatography to give the analytically pure Man-1. ^{1}H NMR (300 MHz, D_2O): δ 5.93−5.84 (m, 1 H), 5.39−5.19 (m, 2 H), 4.81 (d, 1 H, J = 1.2 Hz), 4.03 (d, 2 H, J = 5.7 Hz), 3.90−3.59 (m, 10 H); HRMS-ESI: m/z $C_{11}H_{12}O_7$ $(M + Na)^+$ calcd 287.1107, found 287.1112.

Fabrication of 2-D Lectin Recognition Sensors. We spread the 2-D PS colloidal arrays on a water surface by using the previously reported needle tip flow technique.[11] We transferred the 2-D array on the water surface to a glass slide. Then a solution of AAm, AAc, MBAAm, and Man-1 was layered onto the 2-D array on the glass slide. Another glass slide was placed on top to cover the polymerization solution. The polymerization was carried out by using UV light (365 nm) at room temperature. After 10 min, we peeled the 2-D array hydrogel film from the glass slide and washed it five times in 0.1 M NaCl solutions to remove any unreacted monomers and impurities. The different reaction stoichiometries utilized for the 2-D PhC hydrogel preparations are listed in Table 1.

Table 1. Stoichiometry of PAAm/Mannose Hydrogels[a]

code	AAm (mg)	Man-1 (mg)	MBAAm (mg)	AAc (μL)	initiator (μL)[b]	particle spacing (nm)[c]
M1	40	16	0.4	0	12	N/A[d]
M2	40	16	0.4	8	12	1080
M3	40	8	0.4	0	12	874
M4	40	8	0.4	8	12	1023
M5	40	4	0.4	8	12	998
M6	40	16	0.2	8	12	1389
M7	40	32	0.2	8	12	1802

[a]The total reaction solution volume is 400 μL. [b]The initiator is Irgacure 2959 in DMSO (33%, w:v). [c]Particle spacing is obtained from the Debye diffraction ring. [d]Hydrogel without 2-D particle array.

SEM Characterization. The PS 2-D arrays and the dried 2-D PhC hydrogel sensors were sputter coated with a thin layer of Au, and the surface morphology was determined by using a scanning electron microscope (SEM, JEOL JSM6390LV).

Protein Recognition. To characterize the response of the sensor to proteins, the hydrogel sensors were equilibrated in 0.1 M NaCl solution, and small pieces of the sensor were placed in 0.01 to 2.0 mg/mL Con A solutions containing 0.1 M NaCl. The 2-D sensors were equilibrated overnight before diffraction measurements. Diffraction of the 2-D PhC Man-1 hydrogel sensors was monitored by using an Ocean Optics USB2000-UV-vis spectrometer, a LS-1 tungsten halogen light source, and an R-series fiber optic reflection probe. All diffraction measurements were made with the 2-D array-hydrogels on a silver front surface mirror (Thorlabs, VA). The diffraction measurements were carried out in a Littrow configuration with the fiber at a ∼18° angle from the array normal.[10−14]

Debye ring diffraction was used to monitor the particle spacing.[13] We excited the 2-D PhC Man-1 hydrogel sensor along its normal with a 532 nm green laser pointer. A perfectly ordered hexagonally ordered 2-D array would show diffraction into six hexagonally ordered spots at an angle that depends on the particle spacing. The 2-D arrays in these PhC Man-1 hydrogel sensors consist of orientationally disordered hexagonal domains smaller than the size of the laser beam. Thus, the 2-D particle array diffraction pattern appears as a ring (Figure 1). The first-order diffraction angle, α, depends upon

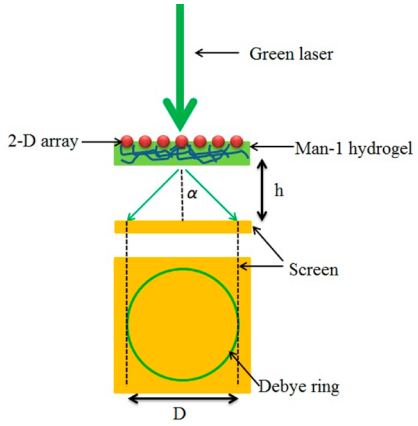

Figure 1. Measurement of Debye diffraction ring diameter. h is the distance between the 2-D array and the screen. D is the diameter of the Debye diffraction ring on the screen. The diffraction angle α is calculated from $\tan \alpha = D/2h$.

the particle spacing: $\sin \alpha = 2\lambda_{laser}/(3^{1/2}d)$, where α is the interior angle of the Debye diffraction ring, λ_{laser} is the laser wavelength, and d is the particle spacing. The diffraction angle α can be determined from the Debye diffraction ring diameter: $\alpha = \tan^{-1}(D/2h)$, where D is the Debye ring diameter and h is the distance between the 2-D array and screen. We easily monitor the 2-D particle spacing:[14]

$$d = \frac{4\lambda_{laser}\sqrt{(D/2)^2 + h^2}}{\sqrt{3}D}$$

To test the reversibility of the 2-D PhC Man-1 hydrogel sensors, we washed a 2-D PhC sensor with 5 mg/mL D-(+)-mannose solution in 0.1 M NaCl (containing 1 mM Ca^{2+} and 0.5 mM Mn^{2+}) at least 5 times over multihour intervals to ensure complete Con A removal. The 2-D PhC sensors were then washed with 0.1 M NaCl aqueous solutions (containing 1 mM Ca^{2+} and 0.5 mM Mn^{2+}) and used to determine 0.5 mg/mL Con A solutions.

RESULTS AND DISCUSSION

Previously, we attached a 2-D array hydrogel containing biotin in a two-step method, where we first polymerized a hydrogel containing *N*-hydroxysuccinimide ester groups for amine coupling. We then reacted EZ-Link amine-PEG_3-biotin with this hydrogel.[14] We found that the grafting efficiency was relatively low.[20] Here we used a more versatile one-step copolymerization method that directly polymerized vinyl-functionalized mannose with AAm and AAc monomers (Figure 2).

We expect that the interaction between Con A and mannose of our hydrogel PhC is similar to that between Con A and methyl α-D-mannopyranoside.[21−23] Con A in solution is a homotetramer of four identical subunits. Each subunit has one saccharide-binding site in a surface shallow pocket,[24] and two

dx.doi.org/10.1021/ac5015854 | Anal. Chem. 2014, 86, 9036−9041

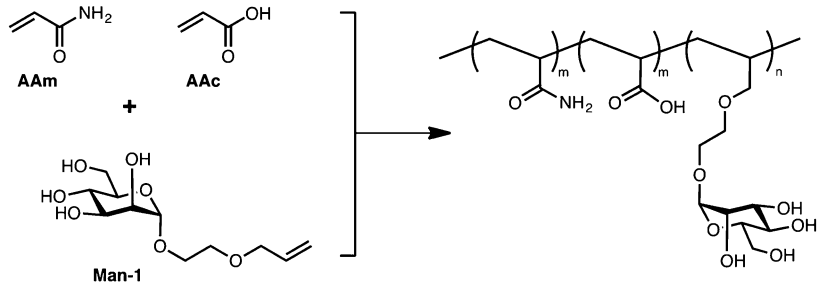

Figure 2. Mannose hydrogels were synthesized through the copolymerization of AAm, AAc, and vinyl-substituted mannose (Man-1) with UV irradiation (λ = 365 nm) for 10 min at room temperature.

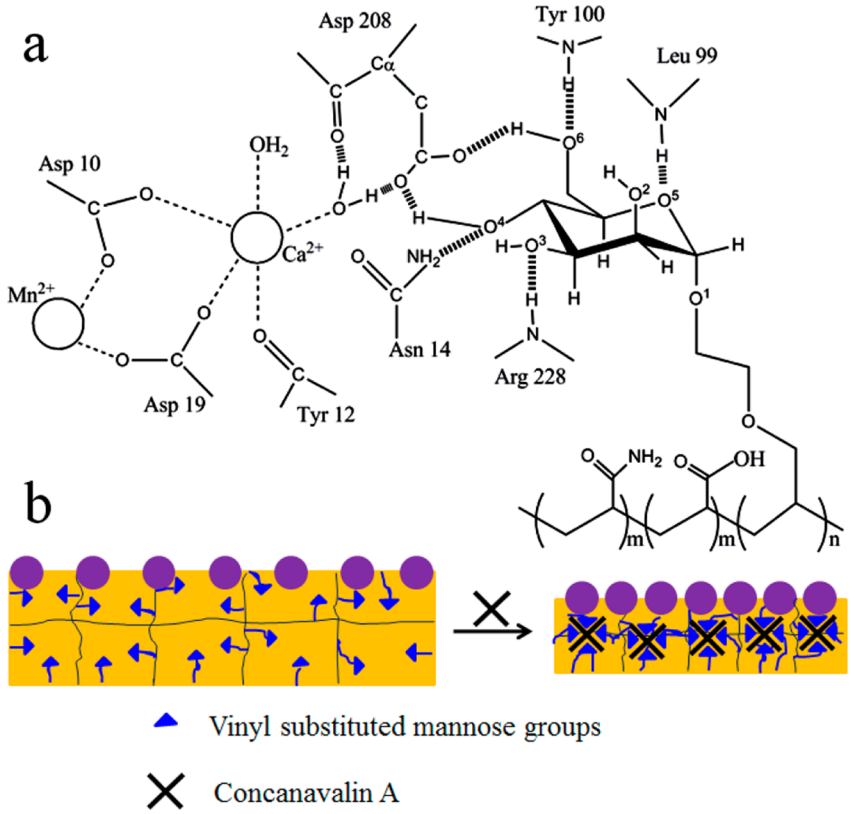

Figure 3. Mechanism of (a) Con A attachment to mannose attached to hydrogel. (b) Shrinkage and particle spacing decrease in Man-1 hydrogel sensor that results from Con A binding.

distinct metal-binding sites: one for a calcium ion and one for a transition-metal ion.[25] Each mannose is bound to Con A by hydrogen bonding and van der Waals interactions. The mannose would be bound in its C1 chair conformation (Figure 3a). Figure 3a shows that O3, O4, O5, and O6 all form cooperative hydrogen bonds. In particular, O4 and O6 form a bidentate hydrogen bond with the carboxylic acid group of Asp 208, and O5 and O6 form a bidentate hydrogen bond with backbone amide N atoms of Leu 99 and Tyr 100.[22] In addition, van der Waals contacts are close in the region of the O3, O4, C6, and O6 mannose. The binding of the hydrogel mannose to Con A forms cross-links that shrink the mannose containing hydrogel and blue-shift the 2-D CCA diffraction (Figure 3b).

Figure 4a shows an SEM image of a 2-D hexagonal particle array that was transferred from the water surface onto a glass slide. Figure 4b,c shows a freshly prepared 2-D array on top of a hydrogel where the region between particles is filled with hydrogel polymer. If we put the hydrogel in water, the hydrogel swells, causing the particle spacing to increase. The close-packed 2-D particle array becomes nonclose packed, as shown in Figure 4d.

Binding of Con A to the hydrogel mannose increases the hydrogel cross-linking such that the 2-D array particle spacing decreases, causing a diffraction blue shift that reports on the Con A concentration. Figure 5a shows the dependence of the diffraction wavelength maximum of the M2 2-D array sensor as a function of the Con A concentration. In the absence of Con A, the 2-D array diffraction maximum occurs at 600 nm as measured in the Littrow configuration. The diffraction wavelength blue shifts with increasing Con A concentrations; at 2 mg/mL, the diffraction blue shifts to 554 nm. The inset photograph in Figure 5a clearly shows the visually evident color changes as the Con A concentrations change. Thus, Con A concentrations can be roughly determined by visually observing diffraction color changes of the sensor.

Figure 5b shows the Con A concentration dependence of the particle spacing of the M2 2-D PhC sensor measured by monitoring the Debye diffraction ring diameter. The particle

dx.doi.org/10.1021/ac5015854 | Anal. Chem. 2014, 86, 9036−9041

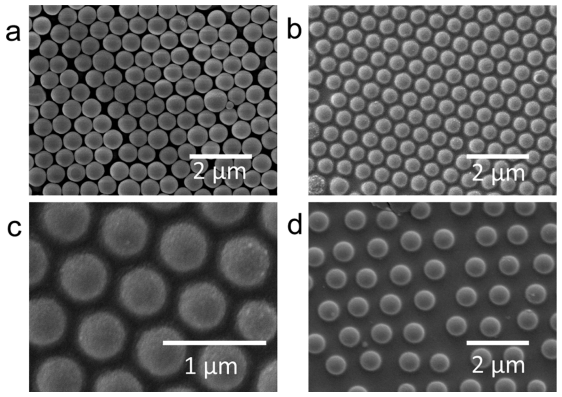

Figure 4. SEM images of (a) PS 2-D array on glass slide. (b and c) PS 2-D array monolayer on top of freshly prepared M2 hydrogel (Table 1). The interstices between neighboring particles are filled with hydrogel polymer. (d) Nonclose packed 2-D array on top of M2 hydrogel swollen in water and then dried in air. Hydrogel swelling causes close-packed structure to expand to become nonclose packed.

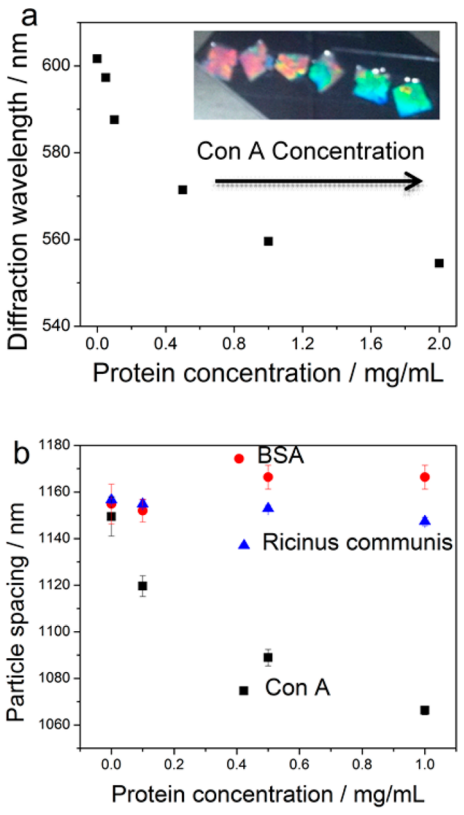

Figure 5. (a) Dependence of normalized diffraction spectra of the M2 2-D mannose hydrogel sensors upon Con A concentration in 0.1 M NaCl aqueous solutions that contain 1 mM Ca^{2+} and 0.5 mM Mn^{2+}. The diffraction is measured in a Littrow configuration with an angle of ~18° between the probe and the 2-D array normal. The inset shows photographs taken in the Littrow configuration where the camera lens axis is at an angle of ~18° from the normal. (b) Con A, Ricinus communis, and BSA concentration dependence of the particle spacing of the M2 2-D PhC sensor.

spacing decreases with increasing Con A concentrations. The spacing change is due to Con A binding as evident from the control experiment where little change occurs in the array spacing upon addition of the protein BSA; proteins that do not bind mannose do not impact the diffraction. The 2-D PhC Man-1 sensor selectively detects the mannose-specific lectin Con A due to its large association constant and its binding selectivity for mannose.[26,27] Figure 5b shows that our mannose PhC sensor has little response to the lectin *Ricinus communis* agglutinin I, that is selective for galactose.[28]

We examined the dependence of the responsivity of our mannose hydrogel PhC by changing the relative concentrations of the hydrogel constituents, AAm, AAc, MBAAm, and Man-1 (Table 1). Figure 6 shows that the M2 composition hydrogel particle spacing decreases 136 nm upon addition of 2 mg/mL

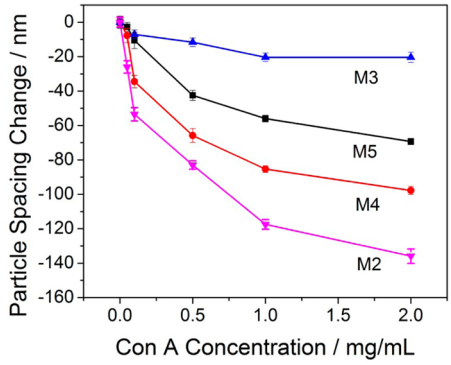

Figure 6. Particle spacing dependence on Con A concentration of the 2-D PhC hydrogel sensors prepared with different amounts of Man-1 and AAc (see Table 1 for compositions).

Con A, in contrast to the much smaller 20 nm particle spacing decrease for the M3 hydrogel that has half the Man-1 content. Part of the M3 decreased sensitivity may result from the lack of AAc that results in a less hydrated, less responsive hydrogel.

The particle spacings of the prepared 2-D PhC increase with the mannose content (compare M2, M4, and M5 in Table 1) because of the increase in hydrogel hydrophilicity. Figure 6 shows that M2 has the largest particle spacing decrease for a Con A concentration of 2 mg/mL compared to M3, M4, and M5 hydrogels. This occurs because the increased Man-1 content in M2 results in increased cross-linking upon Con A binding. As the Man-1 content decreases for M4 and M5, the Con A responsivity decreases.

Table 1 shows that decreasing the hydrogel cross-linker content to 0.5% increases the particle spacing to 1389 nm (M6) because the decreased cross-linking results in a decreased elastic restoring force. This does not result in a significant increase in its Con A sensitivity (Figure 7).

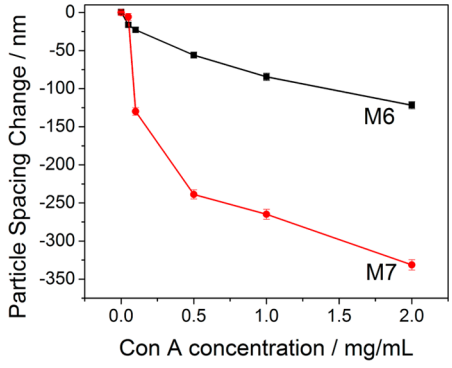

Figure 7. Particle spacing dependence on Con A concentrations of 2-D PhC hydrogel sensors with 16 mg (M6) and 32 mg (M7) Man-1 where the MBAA cross-linker concentration is 0.5%. Higher Man-1 content causes larger Con A-induced particle spacing decrease.

dx.doi.org/10.1021/ac5015854 | *Anal. Chem.* 2014, 86, 9036−9041

A further increase in the Man-1 content dramatically increases the particle spacing to 1802 nm (M7). This increase in the Man-1 content gives rise to a very large increase in Con A sensitivity where M7 shows a 330 nm particle spacing decrease for a 2 mg/mL Con A concentration. We can further increase the 2-D PhC sensitivity by further increasing the Man-1 concentration and decreasing the cross-linker concentration. We calculated the detection limit for the most responsive hydrogel, the M2 sensor, which we calculate to be 0.02 mg/mL (0.7 μM).

We also examined the reversibility of our Con A sensing response. Figure 8 shows the results of five cyclings of our 2-D PhC Man-1 hydrogel sensor (M4) for its response to 0.5 mg/mL of Con A. Little variation in response occurs, and the particle spacings, before and after, Con A addition are relatively constant.

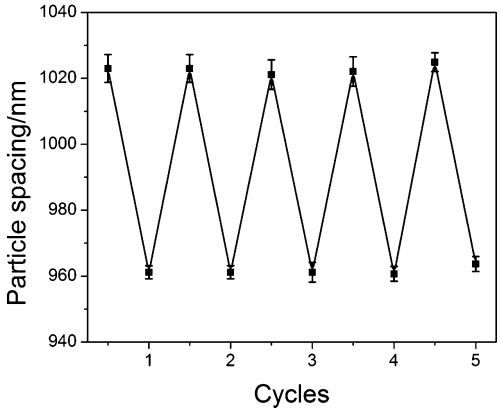

Figure 8. Reversibility of M4 2-D PhC to 0.5 and 0 mg/mL Con A solution.

The kinetics of 2-D PhC Man-1 hydrogel sensor (M5) response to 1 mg/mL Con A is shown in Figure 9. The 2-D hydrogel sensor equilibrates in ~8 h after immersion into the 2 mL 1 mg/mL Con A solution. The faster response over the first 2 h decreases with time. Presumably this slow response is limited by the rate of diffusion of the Con A into the hydrogel and its formation of equilibrium mannose cross-links.

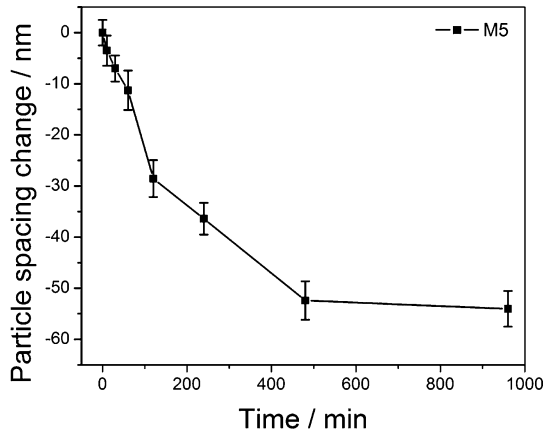

Figure 9. Kinetics of M5 2-D PhC Man-1 hydrogel sensor detection of 1 mg/mL Con A solution.

CONCLUSION

We describe the development of 2-D PhC sensors for selective mannose-specific lectin sensing. 2-D particle array hydrogels were fabricated by polymerizing the reactants on top of self-assembled 2-D particle arrays. Mannose was attached to the hydrogel via an ethoxylethyl linker to induce Con A binding that forms cross-links that shrink the hydrogel volume and decrease the 2-D particle spacing, causing diffraction blue shifts. Increasing the mannose content and decreasing the cross-link density results in an increase of the hydrogel swelling as well as sensor sensitivity. The 2-D PhC mannose hydrogel sensor response is reversible over at least five cycles. This work has demonstrated a new motif for Con A sensing. Further work is in progress to utilize other carbohydrates to sense other lectins and microbial organisms.

AUTHOR INFORMATION

Corresponding Authors

*E-mail: xinyuliu@pitt.edu.

*E-mail: asher@pitt.edu.

Author Contributions

†These authors contributed equally.

Notes

The authors declare no competing financial interest.

ACKNOWLEDGMENTS

The authors gratefully acknowledge HDTRA (grant no. 1-10-1-0044 to S.A.A.) and Department of Chemistry University of Pittsburgh (startup fund to X.L.) for funding support.

REFERENCES

(1) http://www.smartglobalhealth.org/issues/entry/infectious-diseases (Accessed April 10, 2014).

(2) Hemmila, I. *Clin. Chem.* **1985**, *31*, 359−370.

(3) Meulenberg, E. P.; Mulder, W. H.; Stoks, P. G. *Environ. Sci. Technol.* **1995**, *29*, 553−561.

(4) Van Emon, J. M.; Lopez-Avila, V. *Anal. Chem.* **1992**, *64*, 78A−88A.

(5) Dankwardt, A. Immunochemical Assays in Pesticide Analysis. In *Encyclopedia of Analytical Chemistry*; John Wiley & Sons, Ltd: New York, 2006.

(6) Nizet, V, Esko, J. D. Bacterial and Viral Infections. In *Essentials of Glycobiology*, 2nd ed.; Varki, A.; Cummings, R. D.; Esko, J. D.; Freeze, H. H.; Stanley, P.; Bertozzi, C. R.; Hart, G. W.; Etzler, M. E., Eds.; Cold Spring Harbor Laboratory Press: Cold Spring Harbor, NY, 2009; Chapter 39. Available from http://www.ncbi.nlm.nih.gov/books/NBK1952/.

(7) Lin, C.-C.; Yeh, Y.-C.; Yang, C.-Y.; Chen, C.-L.; Chen, G.-F.; Chen, C.-C.; Wu, Y.-C. *J. Am. Chem. Soc.* **2002**, *124*, 3508−3509.

(8) Disney, M. D.; Zheng, J.; Swager, T. M.; Seeberger, P. H. *J. Am. Chem. Soc.* **2004**, *126*, 13343−13346.

(9) Vedala, H.; Chen, Y.; Cecioni, S.; Imberty, A.; Vidal, S.; Star, A. *Nano Lett.* **2011**, *11*, 170−175.

(10) Zhang, J.-T.; Wang, L.; Luo, J.; Tikhonov, A.; Kornienko, N.; Asher, S. A. *J. Am. Chem. Soc.* **2011**, *133*, 9152−9155.

(11) Zhang, J.-T.; Wang, L.; Lamont, D. N.; Velankar, S. S.; Asher, S. A. *Angew. Chem., Int. Ed.* **2012**, *51*, 6117−6120.

(12) Zhang, J.-T.; Smith, N.; Asher, S. A. *Anal. Chem.* **2012**, *84*, 6416−6420.

(13) Zhang, J.-T.; Wang, L.; Chao, X.; Velankar, S. S.; Asher, S. A. *J. Mater. Chem. C* **2013**, *1*, 6099−6102.

(14) Zhang, J.-T.; Chao, X.; Liu, X.; Asher, S. A. *Chem. Commun.* **2013**, *49*, 6337−6339.

(15) Cai, Z.; Zhang, J.-T.; Xue, F.; Hong, Z.; Punihaole, D.; Asher, S. A. *Anal. Chem.* **2014**, *86*, 4840−4847.

(16) Fenzl, C.; Hirsch, T.; Wolfbeis, O. S. *Angew. Chem., Int. Ed.* **2014**, *53*, 3318−3335.

(17) Ge, J.; Yin, Y. *Angew. Chem., Int. Ed.* **2011**, *50*, 1492−1522.

(18) Takeoka, Y. *J. Mater. Chem. C* **2013**, *1*, 6059−6074.
(19) Reese, C. E.; Asher, S. A. *J. Colloid Interface Sci.* **2002**, *248*, 41−46.
(20) Schnaar, R. L.; Lee, Y. C. *Biochemistry* **1975**, *14*, 1535−1541.
(21) Derewenda, Z.; Yariv, J.; Helliwell, J. R.; Kalb, A. J.; Dodson, E. J.; Papiz, M. Z.; Wan, T.; Campbell, J. *EMBO J.* **1989**, *8*, 2189−2193.
(22) Naismith, J. H.; Emmerich, C.; Habash, J.; Harrop, S. J.; Helliwell, J. R.; Hunter, W. N.; Raftery, J.; Kalb, A. J.; Yariv, J. *Acta Crystallogr., Sect D: Biol. Crystallogr.* **1994**, *50*, 847−858.
(23) Loris, R.; Hamelryck, T.; Bouckaert, J.; Wyns, L. *Biochim. Biophys. Acta* **1998**, *1383*, 9−36.
(24) Yariv, J.; Kalb, A. J.; Levitzki, A. *Biochim. Biophys. Acta* **1968**, *165*, 303−305.
(25) Kalb, A. J.; Levitzki, A. *Biochem. J.* **1968**, *109*, 669−672.
(26) Hester, G.; Kaku, H.; Goldstein, I. J.; Wright, C. S. *Nat. Struct. Mol. Biol.* **1995**, *2*, 472−479.
(27) Drickamer, K. *Nat. Struct. Mol. Biol.* **1995**, *2*, 437−439.
(28) Montfort, W.; Villafranca, J. E.; Monzingo, A. F.; Ernst, S. R.; Katzin, B.; Rutenber, E.; Xuong, N. H.; Hamlin, R.; Robertus, J. D. *J. Biol. Chem.* **1987**, *262*, 5398−403.